ELSEVIER

International Journal of Mass Spectrometry 185/186/187 (1999) 707–725

International Journal of Mass Spectrometry

Stepwise solvation of halides by alcohol molecules in the gas phase

Bogdan Bogdanov, Michael Peschke[1], D. Scott Tonner, Jan E. Szulejko, Terry B. McMahon*

Department of Chemistry, University of Waterloo, 200 University Avenue West, Waterloo, Ontario N2L 3G1, Canada

Received 8 July 1998; accepted 26 August 1998

Abstract

The gas phase equilibrium clustering reactions $X^-(ROH)_n + ROH \rightleftharpoons X^-(ROH)_{n+1}$ (X = F, Cl, Br, I; R = CH_3, CH_3CH_2, $(CH_3)_2CH$, $(CH_3)_3C$; $n = 0, 1, 2$) have been investigated by using pulsed-ionization high pressure mass spectrometry (PHPMS). From the corresponding van't Hoff plots the standard enthalpies ($\Delta H^O_{n,n+1}$) and entropies ($\Delta S^O_{n,n+1}$) were obtained, which are discussed in terms of the radii of the halides, the geometry of the alcohol molecules, the number of alcohol molecules, and molecular properties such as polarizability and gas phase acidity. The observed enthalpy trends can be explained on the basis of ion-dipole, ion-induced dipole, and dipole-dipole interactions within the clusters. The observed entropy trends are qualitatively discussed in terms of hindered rotations and low frequency intermolecular vibrations. In general, where available, there is good agreement between the present data and literature values obtained by various experimental techniques. In addition to the experiments, both density functional theory (DFT) calculations at the B3LYP/6–311+G(d,p) level of theory and G2 level calculations have been performed on a number of selected systems to test these methods for obtaining energetic data and to gain more insight into the structures of the investigated clusters. (Int J Mass Spectrom 185/186/187 (1999) 707–725) © 1999 Elsevier Science B.V.

Keywords: Halide alcohol clusters; Thermochemistry; Pulsed-ionization high pressure mass spectrometry; DFT and G2 calculations.

1. Introduction

Over the past three decades the study of both positive and negative gas phase cluster ions has made significant contributions to such diverse fields in science as atmospheric chemistry, gas phase ion chemistry, surface science, and catalysis. The thermochemical data obtained from these gas phase measurements has proved to be very useful. By inference, comparison with condensed phase data may be used to deduce solvent effects.

Halide clusters have been among the most extensively studied systems. This is not surprising considering their common occurrence and importance in organic chemistry, biochemistry, and mass spectrometry. These spherical, noble gas configuration anions form a very sensitive probe for observing trends in ion-molecule interactions. The halide water clusters

* Corresponding author. E-mail: mcmahon@watsci.uwaterloo.ca

[1]Present address: Department of Chemistry, University of Alberta, Edmonton, Alberta T6G 2R3, Canada.

Dedicated to Professor Michael T. Bowers on the occasion of his 60th birthday.

PII S1387-3806(99)14180-5

have been studied particularly well, both experimentally [1–9] and theoretically [10–23]. This is largely because of the fact that water is the most common protic solvent. Alcohols represent a class of protic solvents for which corresponding halide clusters have received a fair amount of interest over the years [3,5–7,9,24–36]. All of these systems show interesting trends in thermochemical data if either the halide, the alcohol ligand, or the number of ligands is changed.

Among experimental techniques used to study the halide protic solvent molecule clusters are high pressure mass spectrometry (HPMS) [1–4], pulsed-ionization high pressure mass spectrometry (PHPMS) [5–9,30], ion cyclotron resonance (ICR) [25,26,37], Fourier transform ion cyclotron resonance mass spectrometry (FT-ICR) [29,31,34,36], electron photo detachment spectroscopy (EPDS) [27,28,33,35], negative ion photoelectron spectroscopy (NIPES) [38–40], infrared multiphoton dissociation (IRMPD) [24,32], and vibrational predissociation spectroscopy (VPDS) [41,42]. In general, reasonable agreement is observed when comparing data from these different experimental techniques.

From quantum mechanical and molecular dynamics computations, considerable insight has been gained into the static structures as well as the energetics and dynamic aspects of halide water clusters [8,10–23,43–48]. On the other hand, only a few papers report work done on halide alcohol clusters [23,30,34,36,38,49].

Surprisingly, thermochemical data for the equilibrium clustering of many halide alcohol systems have never been determined. This is especially true for higher order clusters (more than two solvent molecules) of the fluoride and the heavier halides (Br^- and I^-) with larger alcohol molecules (C_2H_5OH, i-C_3H_7OH, t-C_4H_9OH).

In the present work a systematic study has been performed to obtain new data as well as to evaluate existing thermochemical data. The standard enthalpies (ΔH^o) and entropies (ΔS^o) have been analyzed for trends to gain a clearer understanding of the distinct influences of the halide, the alcohol molecule, and the number of alcohol molecules.

2. Experiment

All measurements were carried out on two pulsed-ionization high pressure mass spectrometers, configured around either a *VG* 8-80 or a reversed *VG* 70-70 (BE geometry) instrument. The instruments, both constructed at the University of Waterloo, have been described in detail previously [50,51]. The general principles and capabilities [52], as well as the limitations [53] of PHPMS have been described in the literature.

Gas mixtures were prepared in a 5 L heated stainless steel reservoir (60 °C–85 °C) by using CH_4 as the bath gas at pressures of 135 Torr–835 Torr. The halides F^-, Cl^-, Br^-, and I^- were generated from NF_3 (0.05%–0.20%), CCl_4 (<0.01%), CH_3Br (0.25%–1.50%) or $CHBr_3$ (<0.01%), and CH_3I (<0.01%), respectively by dissociative electron capture (DEC) of thermalized electrons from 300 μs pulses of a 2 keV electron gun beam.

The four alcohol neutrals (CH_3OH, C_2H_5OH, i-C_3H_7OH, t-C_4H_9OH) were added to give relative partial pressures between 0.01% and 20%, depending on the temperature and the nature of the experiments involved. The ion source pressure and temperature ranged from 3.5 to 10.0 Torr and from 300 to 710 K, respectively.

Time intensity profiles of mass selected ions were monitored by using a PC based multichannel scalar (MCS) data acquisition system, typically configured between 50 and 400 μs dwell time per channel over 250 channels. Additive accumulations of ion signals resulting from 250–2000 electron beam pulses were typically used.

The equilibrium constants (K_{eq}) at different temperatures are determined from Eq. (1).

$$K_{eq} = \frac{\mathrm{Int}(X^-(ROH)_{n+1})}{\mathrm{Int}(X^-(ROH)_n)} \times \frac{P^o}{P_{ROH,source}} \quad (1)$$

In Eq. (1), $\mathrm{Int}(X^-(ROH)_{n+1})/\mathrm{Int}(X^-(ROH)_n)$ is the ion intensity ratio of the $X^-(ROH)_{n+1}$ and $X^-(ROH)_n$ clusters at equilibrium, respectively, P^o is the standard pressure (1 atm), and $P_{ROH,source}$ is the

partial pressure (in atm) of the alcohol in the ion source.

From the equilibrium constants the standard Gibbs' free energy (ΔG^o) at the different absolute temperatures (T) can be calculated from Eq. (2).

By combining Eq. (2),

$$\Delta G^o = -RT \ln K_{eq} \quad (2)$$

and Eq. (3) the van't Hoff Eq. (4) can be obtained.

$$\Delta G^o = \Delta H^o - T\Delta S^o \quad (3)$$

$$\ln K_{eq} = \frac{\Delta S^o}{R} - \frac{\Delta H^o}{R}\frac{1}{T} \quad (4)$$

By plotting $\ln K_{eq}$ versus $1/T$, ΔH^o and ΔS^o can be calculated from the slope and intercept, respectively.

All equilibrium constants obtained were essentially independent of the partial pressures of the alcohols and the ion source pressure. The uncertainties in the enthalpies and entropies were calculated from the standard deviations in the slope and intercept of the van't Hoff plots by statistical procedures.

Most chemicals used were commercially available and used directly without further purification.

For all NF_3/ROH/CH_4 mixtures, an ion with m/z 115 was always present. The relative intensities of m/z 115, 116, and 117 in the mass spectrum suggest that it contains one sulfur atom. This ion has the same m/z value as $F^-(CH_3OH)_3$, and so CD_3OH was used instead of CH_3OH.

3. Computation

Based on a review by Curtiss et al. [54] and previous experience, Becke3LYP was chosen as the standard basis for the computational part of this study. To verify the suitability of the density functional theory (DFT) method for the present chemical systems, the monosolvated halides were compared to G2 results. Chemical accuracy of ± 2.5 kcal mol^{-1} or better compared to experimental data has been claimed for the G2 procedure [54]. The basis set chosen for optimizations and frequency calculations was 6-311+G(d,p) [55]. The large basis set is necessitated by the diffuse nature of the anions. To check the energy dependence on larger basis sets, several single point calculations were done with the 6-311++G(3df,3pd) basis set. All calculations were done with the GAUSSIAN 94 suite of programs [56].

4. Results and discussion

The results for the experimentally determined equilibrium constants (K_{eq}) for the three consecutive stepwise solvation reactions [Eqs. (5)–(7)]

$$(0,1) \quad X^- + ROH \rightleftharpoons X^-(ROH) \quad (5)$$

$$(1,2) \quad X^-(ROH) + ROH \rightleftharpoons X^-(ROH)_2 \quad (6)$$

$$(2,3) \quad X^-(ROH)_2 + ROH \rightleftharpoons X^-(ROH)_3 \quad (7)$$

(X = F, Cl, Br, I; R = Me, Et, *i*-Pr, *t*-Bu) are displayed in the van't Hoff plots in Fig. 1(A) to (H). The numbers in the van't Hoff plots correspond to the system number as shown in Tables 1–5 (see below). The corresponding standard enthalpy and entropy changes, and known literature values are shown in Tables 1–4.

The direct clustering of F^- onto C_2H_5OH, i-C_3H_7OH, and t-C_4H_9OH could not be measured because of the very high binding enthalpies involved. In order to obtain ΔH^o and ΔS^o, F^- exchange reactions involving methanol and the three other alcohols were performed, Eq. (8).

$$F^-(CH_3OH) + ROH \rightleftharpoons F^-(ROH) + CH_3OH \quad (8)$$

By measuring the standard enthalpy and entropy changes for these exchange equilibria and by using earlier experimentally determined ΔH^o and ΔS^o values of F^- clustering onto methanol ($\Delta H^o = -30.5 \pm 0.7$ kcal mol^{-1} and $\Delta S^o = -23.4 \pm 1.2$ cal mol^{-1} K^{-1}) [29], the corresponding thermochemical data of F^- clustering onto ROH (R = Et, *i*-Pr, *t*-Bu) could be obtained experimentally. These values are summarized in Table 5. In Fig. 1 the van't Hoff plots for the clustering of fluoride onto ethanol (4), *iso*-propanol (7), and *tert*-butanol (10) have been

Table 1
Summary of experimental thermochemical data for the fluoride alcohol clustering equilibria $X^-(ROH)_n + ROH \rightleftharpoons X^-(ROH)_{n+1}$ (X = F; R = Me, Et, *i*-Pr, *t*-Bu; $n = 0, 1, 2$)

System No.	X	R	$(n,n+1)$	Present work		Literature value		Method	Reference
				$\Delta H^o_{n,n+1}$ [a]	$\Delta S^o_{n,n+1}$ [b]	$\Delta H^o_{n,n+1}$ [a]	$\Delta S^o_{n,n+1}$ [b]		
1	F	Me	(0,1)			−29.6	−22.6	ICR	[25]
						−30.5 ± 0.7	−23.4 ± 1.2	PHPMS	[29]
						−23.3	−25.0	PHPMS	[30]
						−29.6 ± 0.5		EPDS	[35]
2	F	Me	(1,2)	−20.3 ± 0.3	−24.6 ± 0.8	−19.8 ± 0.3	−22.5 ± 0.8	PHPMS	[29]
						−19.3	−23.2	PHPMS	[30]
3	F	Me	(2,3)	−15.1 ± 0.6	−23.6 ± 1.6	−18.1 ± 0.1	−32.6 ± 0.6	PHPMS	[29]
						−14.5	−21.2	PHPMS	[30]
4	F	Et	(0,1)	−32.4 ± 0.7	−25.7 ± 1.3	−31.5	−24.9	ICR	[25]
5	F	Et	(1,2)	−20.6 ± 0.3	−25.8 ± 0.6	−20.6 ± 0.5	−27.1 ± 1.2	PHPMS	[29]
6	F	Et	(2,3)	−15.6 ± 0.1	−25.1 ± 0.4				
7	F	*i*-Pr	(0,1)	−33.5 ± 0.7	−26.2 ± 1.3	−32.2	−25.6	ICR	[25]
8	F	*i*-Pr	(1,2)	−20.8 ± 0.2	−25.3 ± 0.6				
9	F	*i*-Pr	(2,3)	−17.6 ± 0.2	−31.0 ± 0.7				
10	F	*t*-Bu	(0,1)	−33.4 ± 0.7	−24.8 ± 1.2	−33.3	−26.1	ICR	[25]
11	F	*t*-Bu	(1,2)	−22.0 ± 0.4	−28.2 ± 0.8				
12	F	*t*-Bu	(2,3)	−18.3 ± 1.0	−35.2 ± 2.8				

[a] kcal mol^{-1}.
[b] cal mol^{-1} K^{-1}.

calculated and drawn based on the above discussion and consequently do not contain any experimental data points.

For the $F^- + ROH \rightleftharpoons F^-(ROH)$ clustering equilibria, $-\Delta H^o$ increases in going from R = Me to *t*-Bu. A similar trend has been observed by Larson and McMahon [25]. Their ICR values are slightly lower than the values obtained from this work. As a reference in that work, Kebarle's ΔH^o value for the $F^- + H_2O \rightleftharpoons F^-(H_2O)$ equilibrium obtained by HPMS experiments [1] had been used.

Hiraoka's $-\Delta H^o$ values for the $F^-(H_2O)_n + H_2O \rightleftharpoons F^-(H_2O)_{n+1}$ clustering equilibria ($n = 0, 1$) [8] determined by PHPMS are higher than the HPMS data, indicating that Kebarle's data might be too low. This has been supported by Xanthes et al. from theoretical calculations [47]. They obtained a fluoride onto water binding enthalpy at 300 K of −26.5 ± 0.5 kcal mol^{-1} by using a new parameterization of the fluoride water interaction within a polarizable water model. The results of ab initio calculations at the MP2(4)/aug-cc-pVDZ and MP2/aug-cc-pVTZ levels of theory were used to parameterize the fluoride water interaction (−26.7 kcal mol^{-1}).

A previous ΔH^o value from this laboratory (−30.5 ± 0.7 kcal mol^{-1}) determined by PHPMS for the F^- onto CH_3OH clustering is in reasonable agreement with Larson and McMahon's ICR data, while Hiraoka's value for the same reaction definitely seems anomalous.

The electrostatic interaction between a halide and an alcohol molecule, $V(r)$, can be described by an ion-dipole and ion-induced dipole model [57,58], Eq. (9),

$$V(r) = \frac{-\mu_D\, q\, \cos\,\theta(r)}{r^2} + \frac{-\alpha\, q^2}{2r^4} \tag{9}$$

From the data in Table 6 it can be concluded that the ion-induced dipole term is mainly responsible for the increase in $-\Delta H^o$ for R = Me to *t*-Bu, despite the r^{-4} dependence. Going from CH_3OH to *t*-C_4H_9OH, the permanent electric dipole moment (μ_D) changes only slightly, whereas the polarizability of the alcohols (α) increases from 3.32 to 8.82 $Å^3$ [59,60]. A plot

Table 2
Summary of experimental thermochemical data for the chloride alcohol clustering equilibria $X^-(ROH)_n + ROH \rightleftharpoons X^-(ROH)_{n+1}$ (X = Cl; R = Me, Et, *i*-Pr, *t*-Bu; $n = 0, 1, 2$)

System No.	X	R	$(n,n+1)$	Present work		Literature value		Method	Reference
				$\Delta H^o_{n,n+1}$ [a]	$\Delta S^o_{n,n+1}$ [b]	$\Delta H^o_{n,n+1}$ [a]	$\Delta S^o_{n,n+1}$ [b]		
13	Cl	Me	(0,1)	−17.5 ± 0.3	−24.0 ± 0.7	−14.1	−14.8	HPMS	[2]
						−14.2	−14.8	HPMS	[3]
						−16.8	−22.9	ICR	[26]
						−17.5 ± 0.1	−22.0 ± 0.2	PHPMS	[4]
						−17.4	−24.1	PHPMS	[7]
						−17.1 ± 0.1	−22.6 ± 0.1	PHPMS	[9]
						−18.7 ± 0.5		EPDS	[35]
14	Cl	Me	(1,2)	−14.1 ± 0.4	−22.8 ± 1.1	−13.0	−19.4	HPMS	[3]
						−14.1	−22.0	PHPMS	[7]
						−13.7 ± 0.2	−22.0 ± 0.5	PHPMS	[9]
15	Cl	Me	(2,3)	−11.5 ± 0.2	−21.6 ± 0.6	−12.3	−23.6	HPMS	[3]
						−11.8	−22.9	PHPMS	[7]
						−10.8 ± 0.3	−22.7 ± 0.8	PHPMS	[9]
16	Cl	Et	(0,1)	−17.9 ± 0.4	−24.3 ± 0.9	−17.3	−23.1	ICR	[26]
						−17.6	−23.7	PHPMS	[7]
17	Cl	Et	(1,2)	−15.3 ± 0.2	−26.7 ± 0.5	−16.1	−25.9	PHPMS	[7]
18	Cl	Et	(2,3)	−13.9 ± 0.7	−29.3 ± 2.1	−12.8	−25.8	PHPMS	[7]
19	Cl	*i*-Pr	(0,1)	−19.4 ± 0.2	−27.1 ± 0.5	−17.6	−23.2	ICR	[26]
						−18.3	−24.7	PHPMS	[7]
20	Cl	*i*-Pr	(1,2)	−16.7 ± 0.3	−30.3 ± 0.7	−15.6	−25.0	PHPMS	[7]
21	Cl	*i*-Pr	(2,3)	−14.9 ± 0.5	−32.2 ± 1.4	−12.5	−26.1	PHPMS	[7]
22	Cl	*t*-Bu	(0,1)	−20.2 ± 0.4	−28.9 ± 1.0	−14.2	−10.3	HPMS	[2]
						−19.2	−27.0	PHPMS	[89]
						−18.1	−23.4	ICR	[26]
						−19.8	−27.4	PHPMS	[7]
23	Cl	*t*-Bu	(1,2)	−16.9 ± 0.2	−32.0 ± 0.5	−14.9	−25.8	PHPMS	[7]
24	Cl	*t*-Bu	(2,3)	−15.8 ± 0.3	−36.0 ± 0.9	−13.7	−31.0	PHPMS	[7]

[a] kcal mol^{-1}.
[b] cal mol^{-1} K^{-1}.

of α versus $-\Delta H^o_{0,1}$ (X^-/ROH) confirms the expected linear relationship (Fig. 2).

The deprotonation enthalpies (ΔH_{acid}) of CH_3OH to *t*-C_4H_9OH are larger than that of HF (Table 6), so that $ROH \cdots F^-$ is a qualitatively correct description for these systems as shown by Mihalick et al. from EPDS experiments of fluoride alcohol adducts [33]. In addition to this, IRMPD experiments of $(CH_3OH)\,F^-$ in a FT-ICR instrument have confirmed that $F^- + CH_3OH$ is indeed the lowest energy dissociation channel [24]. Low kinetic energy collision-induced dissociation (CID) experiments by Wilkinson et al. in a FT-ICR instrument showed that for $(ROH)F^-$ adducts, for which the gas phase acidity of the alcohol molecule is very close to the gas phase acidity of HF, both F^- and RO^- product ions were observed [31]. This was explained by assuming a double well potential energy surface with a very low barrier for proton transfer when $\Delta\Delta H_{acid} \approx 0$ kcal mol^{-1}, whereas for larger $\Delta\Delta H_{acid}$ values, the potential energy surface converts into a single well. This hypothesis has been confirmed by high level ab initio calculations [38,49]. A linear relationship between the gas phase acidity difference of ROH and HF, and the binding enthalpy of F^- (ROH) was established by Larson and McMahon [25]. In Fig. 3 it can be seen that this relationship also applies to the other three halides. This relationship might indicate the existence of a single well potential energy surface as shown in Fig. 4. A similar kind of potential energy surface was suggested by

Table 3
Summary of experimental thermochemical data for the bromide alcohol clustering equilibria $X^-(ROH)_n + ROH \rightleftharpoons X^-(ROH)_{n+1}$ (X = Br; R = Me, Et, *i*-Pr, *t*-Bu; $n = 0, 1, 2$)

System No.	X	R	$(n,n+1)$	Present work $\Delta H^o_{n,n+1}$ [a]	Present work $\Delta S^o_{n,n+1}$ [b]	Literature value $\Delta H^o_{n,n+1}$ [a]	Literature value $\Delta S^o_{n,n+1}$ [b]	Method	Reference
25	Br	Me	(0,1)	−14.5 ± 0.1	−21.9 ± 0.4	−13.9	−17.6	PHPMS	[30]
						−15.1 ± 0.4		EPDS	[35]
26	Br	Me	(1,2)	−12.0 ± 0.2	−21.4 ± 0.5	−12.5	−20.7	PHPMS	[30]
27	Br	Me	(2,3)	−9.5 ± 0.5	−17.6 ± 1.6	−10.6	−21.6	PHPMS	[30]
28	Br	Et	(0,1)	−14.1 ± 0.2	−19.8 ± 0.4	−14.4		FT-ICR	[34]
						−15.2 ± 0.6		EPDS	[35]
29	Br	Et	(1,2)	−11.5 ± 0.6	−19.4 ± 1.8				
30	Br	Et	(2,3)	−9.5 ± 0.3	−17.2 ± 0.9				
31	Br	*i*-Pr	(0,1)	−14.4 ± 0.2	−20.3 ± 0.6	−14.6		FT-ICR	[34]
						−16.5 ± 1.2		EPDS	[35]
32	Br	*i*-Pr	(1,2)	−12.3 ± 0.3	−23.0 ± 0.8				
33	Br	*i*-Pr	(2,3)	−11.5 ± 0.8	−23.6 ± 2.4				
34	Br	*t*-Bu	(0,1)	−15.8 ± 0.2	−24.2 ± 0.5				
35	Br	*t*-Bu	(1,2)	−12.9 ± 0.4	−24.3 ± 1.2				
36	Br	*t*-Bu	(2,3)	−11.6 ± 0.5	−24.4 ± 1.6				

[a] kcal mol^{-1}.
[b] cal mol^{-1} K^{-1}.

Yang et al. [35], although they did not propose any linearity or extension to larger alcohol molecules.

The $F^-(CH_3OH)$ adduct has been studied by high level theoretical calculations a number of times. In Table 7 can be seen that the present B3LYP/6-311+G(d,p) and G2 calculations have been able to reproduce the experimental PHPMS data reasonably well (−31.3 and −29.3 versus −30.5 ± 0.7 kcal · mol^{-1} for ΔH^o, and −22.6 and −21.7 versus −23.4 ± 1.2 cal mol^{-1} K^{-1} for ΔS^o). In general,

Table 4
Summary of experimental thermochemical data for the iodide alcohol clustering equilibria $X^-(ROH)_n + ROH \rightleftharpoons X^-(ROH)_{n+1}$ (X = I; R = Me, Et, *i*-Pr, *t*-Bu; $n = 0, 1, 2$)

System No.	X	R	$(n,n+1)$	Present work $\Delta H^o_{n,n+1}$ [a]	Present work $\Delta S^o_{n,n+1}$ [b]	Literature value $\Delta H^o_{n,n+1}$ [a]	Literature value $\Delta S^o_{n,n+1}$ [b]	Method	Reference
37	I	Me	(0,1)	−11.9 ± 0.2	−20.6 ± 0.5	−11.3	−17.8	PHPMS	[5]
						−11.2	−17.1	PHPMS	[30]
						−14.4 ± 0.4		EPDS	[35]
38	I	Me	(1,2)	−9.5 ± 0.2	−17.6 ± 0.5	−11.1	−22.6	PHPMS	[30]
39	I	Me	(2,3)	−7.7 ± 0.6	−14.4 ± 1.9	−9.8	−22.4	PHPMS	[30]
40	I	Et	(0,1)	−13.0 ± 0.2	−23.1 ± 0.7	−12.1	−18.9	PHPMS	[5]
						−11.7		FT-ICR	[34]
41	I	Et	(1,2)	−10.5 ± 0.2	−20.4 ± 0.6				
42	I	Et	(2,3)	−8.4 ± 0.5	−16.4 ± 1.4				
43	I	*i*-Pr	(0,1)	−13.1 ± 0.2	−22.7 ± 0.6	−12.2	−19.1	PHPMS	[5]
44	I	*i*-Pr	(1,2)	−11.0 ± 0.3	−21.3 ± 0.8				
45	I	*i*-Pr	(2,3)	−9.5 ± 0.7	−20.0 ± 2.2				
46	I	*t*-Bu	(0,1)	−13.1 ± 0.3	−23.3 ± 0.9	−12.1	−18.7	PHPMS	[5]
47	I	*t*-Bu	(1,2)	−11.3 ± 0.4	−23.4 ± 1.1				
48	I	*t*-Bu	(2,3)						

[a] kcal mol^{-1}.
[b] cal mol^{-1} K^{-1}.

Table 5
Summary of experimental thermochemical data for the fluoride alcohol exchange equilibria $X^-(CH_3OH) + ROH \rightleftharpoons X^-(ROH) + CH_3OH$ (X = F; R = Et, *i*-Pr, *t*-Bu)

System No.	X	R	Present work		Literature value		Method	Reference
			ΔH^{o} [a]	ΔS^{o} [b]	ΔH^{o} [a]	ΔS^{o} [b]		
49	F	Et	−1.9 ± 0.2	−2.3 ± 0.4	−1.9	−2.3	ICR	[25]
50	F	i = Pr	−3.0 ± 0.2	−2.8 ± 0.4	−2.7	−3.0	ICR	[25]
51	F	t = Bu	−2.9 ± 0.1	−1.4 ± 0.1	−3.7	−3.5	ICR	[25]

[a] kcal mol^{-1}.
[b] cal mol^{-1} K^{-1}.

the G2 values are in excellent agreement with the experimental results, differing by 1.5 kcal mol^{-1} or less, which is well within the reported accuracy of 2–3 kcal mol^{-1}. In comparison, the DFT results fared slightly worse overall. At the 6-311+G(*d*,*p*) level, the enthalpies at 298 K vary from 0.8 to 2.8 kcal mol^{-1} from experiments, whereas the single point calculations at the 6-311++G(3*df*,3*pd*) level differ from 1.9 to 2.5 kcal mol^{-1}. The agreement is, however, still excellent and well within the expected error bars. The higher level single point calculations do not improve the results significantly, indicating

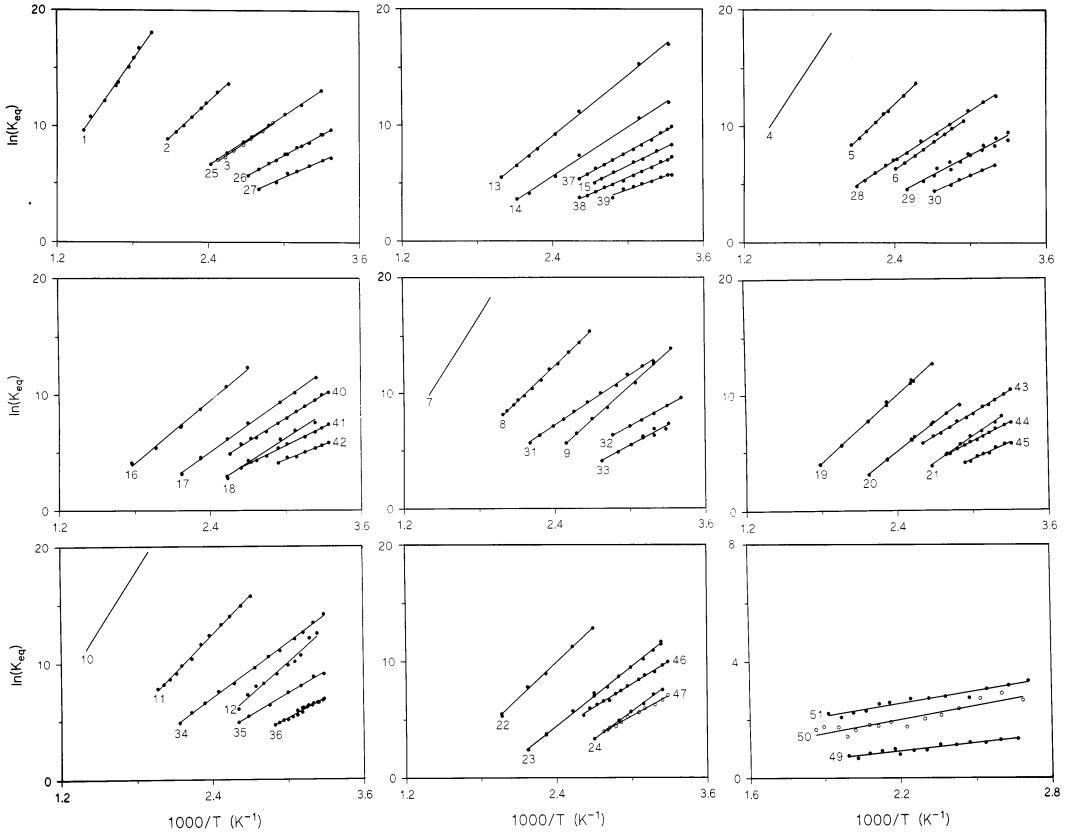

Fig. 1. van't Hoff plots [ln (K_{eq}) versus 1000/*T*] for the stepwise clustering reactions of halides onto alcohols, from which ΔH^{o} and ΔS^{o} for the clustering reactions can be obtained. See Tables 1 to 5 for the specific association reactions referred to in Fig. 1.

Table 6
Standard heat of formation ($\Delta_f H^o$), deprotonation enthalpy (ΔH_{acid}), polarizability (α), radius (r), and permanent electric dipole moment (μ_D) of the halides, alcohols, and corresponding conjugated acids and bases studied in the present work. Data from various sources [59,60,68,69,90]

	$\Delta_f H^o$ [a]	ΔH_{acid} [a]	α [b]	r [c]	μ_D [d]
HF	−65.1	371.2	2.46		1.83
F^-	−59.5		1.47	1.33	
HCl	−22.0	333.2	2.63		1.11
Cl^-	−54.2		4.00	1.81	
HBr	−8.6	322.2	3.61		0.83
Br^-	−50.9		5.25	1.96	
HI	−6.3	314.1	5.35		0.45
I^-	−44.9		7.60	2.20	
CH_3OH	−48.2	381.0	3.32		1.70
CH_3O^-	−33.2				
C_2H_5OH	−56.1	377.1	5.11		1.69
$C_2H_5O^-$	−44.4				
i-C_3H_7OH	−65.2	375.2	6.97		1.66
i-$C_3H_7O^-$	−55.4				
t-C_4H_9OH	−7.8	374.3	8.82		1.66
t-$C_4H_9O^-$	−65.7				

[a] kcal mol^{-1}.
[b] Å^3.
[c] Å.
[d] D.

that the standard 6-311+G(d,p) basis set may give values close to the complete basis set limit for these systems and consequently the highest level single point energies for the rest of the systems were not always obtained.

Hiraoka's value of −26.2 kcal mol^{-1}, obtained by performing low level calculations at the HF/3-21G+p(0.074) level of theory, seems too low [30]. Bradforth et al. performed high level ab initio calculations at the RMP2/6-31++G**//RMP2/6-31++G** and RMP4/6-31++G**//RMP2/6-31++G** levels of theory and obtained fluoride to methanol standard binding enthalpies of −28.9 and −29.5 kcal mol^{-1}, respectively [38]. These values are in excellent agreement with Larson's and McMahon's ICR data and the Yang et al. EPDS data [25,35]. The structures of the monosolvated halide alcohol clusters calculated in this work are very similar to structures from previous computational work.

Wladkowski et al. performed an extensive study on the (CH_3OH) F^- proton-transfer surface [49]. At the MP2/[13s8p6d4f,8s6p4d](+)(492) level of theory, they calculated a value of −30.4 kcal · mol^{-1}, in excellent agreement with earlier experimental work from this laboratory [29].

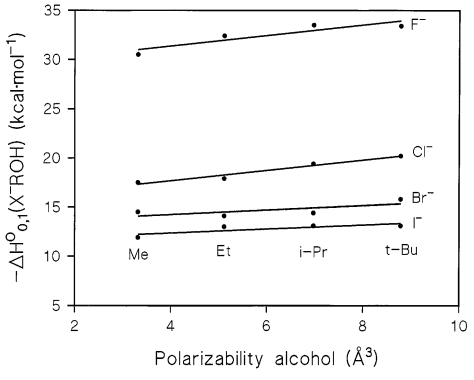

Fig. 2. Alcohol neutral polarizability (α) versus the negative standard enthalpy change for the X^- onto ROH association reactions ($-\Delta H^o_{0,1}(X^-ROH)$).

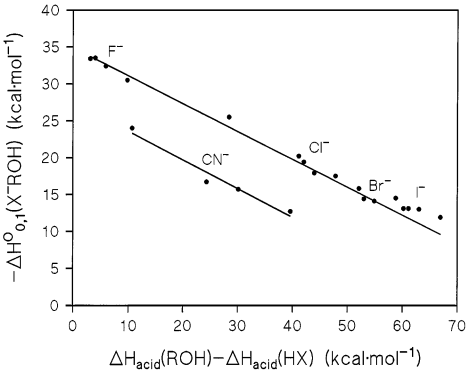

Fig. 3. Deprotonation enthalpy difference (ΔH_{acid}(ROH) − ΔH_{acid}(HX)) versus the negative standard enthalpy change for the X^- onto ROH association reactions ($-\Delta H^o_{0,1}(X^-ROH)$).

Wladkowski et al. performed an extensive study on the (CH_3OH) F^- proton-transfer surface [49]. At the MP2/[13s8p6d4f,8s6p4d](+)(492) level of theory, they calculated a value of −30.4 kcal · mol^{-1}, in excellent agreement with earlier experimental work from this laboratory [29].

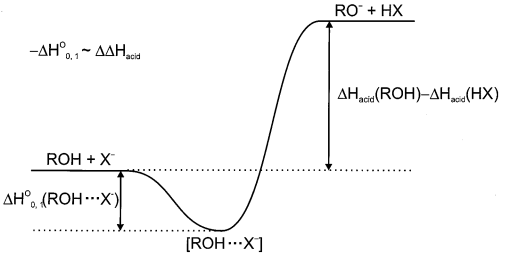

Fig. 4. Single well potential energy surface for the halide alcohol adducts, indicating the linear relationship shown in Fig. 3.

Table 7
Summary of calculated thermochemical data for some selected halide alcohol clustering equilibria ″ = B 3LYP/6-311+G(*d*,*p*).

X	ROH	(*n*,*n*+1)	Method	$\Delta H^{o}_{0\ K}$ [a]	$\Delta H^{o}_{298\ K}$ [a]	ΔS^{o} [b]
F	CH_3OH	(0,1)	B3LYP/6-311+G(*d*,*p*)	−30.9	−31.3	−22.6
			B3LYP/6-311++G(3*df*,3*pd*)//″	−32.0	−32.4	
			G2	−28.7	−29.3	−21.7
F	CH_3OH	(1,2–2)	B3LYP/6-311+G(*d*,*p*)	−20.2	−19.5	−23.4
			B3LYP/6-311++G(3*df*,3*pd*)//	−19.7	−19.0	
Cl	CH_3OH	(0,1)	B3LYP/6-311+G(*d*,*p*)	−14.6	−14.7	−19.2
			B3LYP/6-311++G(3*df*,3*pd*)//″	−14.9	−15.0	
			G2	−15.7	−16.0	−19.5
Cl	CH_3OH	(1,2–2)	B3LYP/6-311+G(*d*,*p*)	−12.2		
			B3LYP/6-311++G(3*df*,3*pd*)//″	−12.2		
Cl	CH_3OH	(1,2–1)	B3LYP/6-311+G(*d*,*p*)	−11.4	−10.7	−29.6
Br	CH_3OH	(0,1)	B3LYP/6-311+G(*d*,*p*)	−12.2	−12.3	
			G2	−13.2	−13.5	−19.5
Br	C_2H_5OH	(0,1)	B3LYP/6-311+G(*d*,*p*)	−12.2	−12.3	−20.0

[a] kcal mol^{-1}.
[b] cal mol^{-1} K^{-1}.

In general, experimentally determined entropy changes may give some additional information on structural features in gas phase cluster ions. Good illustrative examples are the occurrence of bidentate clustering of α,ω-diols onto chloride [61] and the existence of electrostatic and covalent bound isomers of the *tert*-butyl cation clusters with small organic molecules at different temperatures [62]. In general, the variations for the observed entropy changes can be attributed to internal rotational and vibrational contributions on the entropy [63]. The internal rotational contribution may arise from hindered rotations of methyl groups. Wladkowski et al. calculated the $–CH_3$ internal rotation in neutral methanol with a scaled quantum mechanical (SQM) force field method to be 269 cm^{-1} with an infrared intensity of 126.0 (a.u.). [49]. In (CH_3OH) F^- the same rotation was calculated to be at 75 cm^{-1} (IR intensity 0.2). (77 cm^{-1} at the RMP2/6-31++G** level of theory [38]). This result indicates that the $–CH_3$ rotation in (CH_3OH) F^- is less hindered. At the temperatures used in this work, the $–CH_3$ rotor can be considered to be an almost free rotor; the rotational barrier in CH_3OH equals 1.1 kcal mol^{-1}, whereas in (CH_3OH) F^- it is 0.5 kcal mol^{-1} [49]. Comparing R = Me to R = Et to *t*-Bu, the interaction between F^- and methyl groups should become somewhat more accessible, mainly because of the more favorable mutual orientation. One might speculate that this will decrease the contribution to the rotational entropy. In general, vibrations with a frequency smaller than 200 cm^{-1} have very large contributions to the vibrational entropy. The F^- in-plane bend vibration was calculated to be 177 cm^{-1} (IR intensity 18.6) and it is one of the three new vibrations appearing upon formation of the (CH_3OH) F^- complex (167 cm^{-1} at the RMP2/6-31++G** level of theory [38]). It is very likely that the F^- in-plane bend vibration will shift to lower frequencies when R is changed from Me to *t*-Bu, mainly because of the stronger binding enthalpy. This will lead to a larger vibrational entropy. Unfortunately, no similar data are available on (ROH) F^- clusters (R = Et, *i*-Pr, *t*-Bu).

The experimentally determined standard entropy change of -23.4 ± 1.2 cal mol^{-1} K^{-1} is in quite good agreement with the estimated value of −22.6 by Larson and McMahon, and Hiraoka's PHPMS value of −25.0 cal mol^{-1} K^{-1} [25,30]. For the three other alcohols, the standard entropy changes for the F^- + ROH $\rightleftharpoons$ F^-(ROH) clustering equilibria are close to the values suggested by Larson and McMahon within the statistical uncertainty.

At the DFT B3LYP/6-311+G(*d*,*p*) level of theory, a standard entropy of −22.6 cal mol^{-1} K^{-1} was

calculated, which is in good agreement with the experimental value of -23.4 cal mol^{-1} K^{-1}. The DFT method used treats all potential rotors as vibrations. The G2 result of -21.7 cal mol^{-1} K^{-1} deviates more from the experimental value than the DFT value.

For the $F^-(ROH) + ROH \rightleftharpoons F^-(ROH)_2$ equilibrium clustering reactions, in Table 1 it can be seen that $\Delta H^o_{1,2}$ becomes slightly more negative going from R = Me to *t*-Bu. This same trend was observed for $\Delta H^o_{0,1}$. In absolute magnitude, $\Delta H^o_{1,2}$ is considerably smaller than $\Delta H^o_{0,1}$.

$\Delta H^o_{1,2}$ for F^-/CH_3OH of -20.3 ± 0.3 kcal mol^{-1} is in reasonable agreement with Hiraoka's value of -19.3 kcal mol^{-1} and earlier data from this laboratory [29,30]. For the other three alcohols no $\Delta H^o_{1,2}$ values are available in the literature. The consistency in the observed trends is a good indication that the $\Delta H^o_{1,2}$ values are of the correct magnitude. The main reason for the smaller ΔH^o values of the $F^-(ROH) + ROH \rightleftharpoons F^-(ROH)_2$ clustering equilibria, compared to $F^- + ROH \rightleftharpoons F^-(ROH)$, can be found in the increased dipole-dipole interaction and steric effects between the alkyl groups [64]. The dipole-dipole interaction is expected to be the main factor and repulsion will be largest for F^- and smallest for I^-. This observation can be understood by the fact that the alcohol molecules will be closer together when bonded to F^- instead of I^-. Except for the $F^-(ROH)$ complexes, no charge transfer from the halide to the alcohol molecule is expected. Even though the gas phase acidity of CH_3OH is larger than the gas phase acidity of HF, some charge transfer occurs. Wladkowski et al. performed a restricted Hartree–Fock (RHF) Mulliken population analysis at the TZ(+)(*d*,*p*) level of theory [49], shown in Fig. 5. In this case the effective charge on F^- in the $F^-(CH_3OH)$ complex is somewhat smaller than on a bare fluoride. It is reasonable to assume that for $F^-(ROH)$ (R = Et, *i*-Pr, *t*-Bu) the charge transfer will be larger than for $F^-(CH_3OH)$. In the $X^-(ROH)$ clusters (X = Cl, Br, I), all charge will reside on the halide. The effective halide charge, *q*, will remain near -1.00 a.u. in all cases and the dipole-dipole interaction will probably, depending on

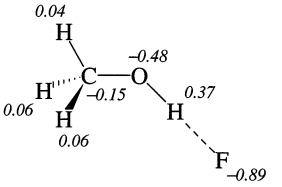

Fig. 5. TZ(+)(*d*,*p*) RHF Mulliken population analysis of $F^-(CH_3OH)$ taken from [49].

the relative orientations among the alcohol molecules, increase even further if another alcohol molecule is added.

The geometries for the disolvated clusters ($F^-(CH_3OH)_2$ and $Cl^-(CH_3OH)_2$), which might be expected to be the lowest in energy, are structures with the halide in the center and the two methanol molecules at opposite sides. Such a starting geometry for $F^-(CH_3OH)_2$ leads to binding energies that are in good agreement with experimental values (between 0.8 and 1.3 kcal mol^{-1}). The structure with the central halide seems therefore to be confirmed. However, it was noted during the optimization cycle that the potential energy surface was quite flat and optimization did not proceed without difficulties. In fact, for the analogous $Cl^-(CH_3OH)_2$ case, the final structure shows two imaginary frequencies of 8*i* and 7*i* cm^{-1}. The very small values for the frequencies shows that the curvature of the "hill top" is almost flat and might be a computational artefact rather than a real feature of the potential energy surface [65–67]. Even for the $F^-(CH_3OH)_2$ case, three frequencies of less than 25 cm^{-1} exist, showing that, for both halides, fairly unhindered torsional and rotational motions are possible.

Kebarle's HPMS data for fluoride water clusters shows a similar trend as for the corresponding alcohol clusters. The observed decrease going from (0, 1) to (1, 2) is not as large as that for the fluoride alcohol clusters [1]. Hiraoka's ΔH^o value of -19.2 ± 0.5 kcal mol^{-1} for H_2O clustering onto $F^-(H_2O)$ seems unusually large compared to the corresponding alcohol values of the present work [8]. The larger than expected value may be because of the internal hydrogen bonding that is present even when both water molecules directly interact with the fluoride [47]. To

Table 8
Summary of calculated vibrational frequencies for fluoride and chloride water clusters

Cluster	Theory	Harmonic frequency (cm^{-1})						Reference
		ω_1	ω_2	ω_3	ω_4	ω_5	ω_6	
$F^-(H_2O)$	MP2/aug-cc-pVDZ	387	563	1135	1694			[45]
$Cl^-(H_2O)$	MP2/aug-cc-pVDZ	187	355	730	1666			[48]
	DFT/DZVP	221	320	763	1703			[89]
$I^-(H_2O)$	MP2/(TZ+P)	111	174	561	1694			[41]
$F^-(H_2O)_2$	MP2/aug-cc-pVDZ	28	31					[45]
$Cl^-(H_2O)_2$	MP2/aug-cc-pVDZ	96	154	178				[48]
	DFT/DZVP	103	167					[89]
$F^-(H_2O)_3(p)$	MP2/aug-cc-pVDZ	59	59	71				[45]
$F^-(H_2O)_3(r)$	MP2/aug-cc-pVDZ	49	78	147	194	199		[45]
$Cl^-(H_2O)_3(p)$	MP2/aug-cc-pVDZ	96 [2]	128	163 [2]				[48]
	DFT/DZVP	101	141	174				[89]
$Cl^-(H_2O)_3(r)$	MP2/aug-cc-pVDZ	39	59	146	178	185	200	[48]

p = pyramidal isomer
r = ring isomer
ω_1 = intermolecular stretch
ω_2 = water in plane rotation
ω_3 = out-of-plane motion $H \cdots X^-$
ω_4 = water bend
ω_5 = "hydrogen bonded" OH stretch
ω_6 = "free" OH stretch

illustrate this, Xantheas et al. calculated ΔH^o at 300 K for the $F^-(H_2O) + H_2O \rightleftharpoons F^-(H_2O)_2$ equilibrium clustering reaction to be -21.6 ± 0.4 kcal mol^{-1} [47], more exothermic than values by Kebarle and Hiraoka [1,8].

The general observed trend in $-\Delta S^o$ for the $F^-(ROH) + ROH \rightleftharpoons F^-(ROH)_2$ clustering equilibria shows a small increase going from R = Me to *t*-Bu. An identical trend is observed for Hiraoka's F^-/CH_3OH/(1,2) PHPMS experiments [30]. In Table 9 an overview is given of the calculated entropy changes and the individual components (translational, rotational, and vibrational entropy changes).

At the MP2/aug-cc-pVDZ level of theory Xantheas et al. calculated the harmonic vibrational frequencies of the $F^-(H_2O)$ (C_S) and $F^-(H_2O)_2$ (C_1) clusters. The intermolecular $F^- \cdots H$–OH stretch and water in-plane wagging motion in $F^-(H_2O)$ are 387 and 563 cm^{-1}, respectively [45]. In Table 8 it can be seen that for the $F^-(H_2O)_2$ cluster, these frequencies have shifted to 28 and 31 cm^{-1}, respectively. These shifts in the vibrational frequencies will make a large contribution to the entropy change. This example nicely illustrates that something similar might be very likely when comparing $F^-(CH_3OH)$ and $F^-(CH_3OH)_2$.

For the $F^-(ROH)_2 + ROH \rightleftharpoons F^-(ROH)_3$ clustering equilibria, similar trends are observed as for the corresponding (1, 2) equilibria. $-\Delta H^o_{2,3}$ increases going from R = Me to *t*-Bu and all values are smaller than $-\Delta H^o_{1,2}$.

The small size of fluoride (Table 6) will cause the alcohol molecules to be closer together than for the other three halides. For R = Et, *i*-Pr, and *t*-Bu no reference data are available in the literature. The experimental HPMS and PHPMS data by Kebarle and Hiraoka on $F^-(H_2O)_n$ show similar trends as the present work [1,8]. Compared to theoretical work at 300 K by Xantheas et al., these experimental results seem too low [47].

No real discussion can be given on the entropy effects for the (2,3) clustering. As mentioned before, hindered rotations and low frequency vibrations are likely the main sources for the observed entropy variations. At the MP2/aug-cc-pVDZ level of theory, the intermolecular $F^- \cdots H$–OH stretch and the water

in-plane rotation have been calculated to be both 59 cm^{-1} [45]. The out-of-plane motion of the hydrogen atom bonded to fluoride has been shifted from 1135 cm^{-1} in $F^-(H_2O)$, to 236 cm^{-1} in $F^-(H_2O)_2$, to 71 cm^{-1} in $F^-(H_2O)_3$, so this vibrational contribution to the entropy change thus increases with increasing cluster size [45]. It needs to be emphasized that the trends observed for the fluoride water clusters will very likely be different than the corresponding alcohol clusters. This is mainly caused by the extra hydrogen bond per water molecule. Nevertheless, the knowledge obtained from these systems has been a starting point for the entropy discussion on fluoride alcohol clusters.

Analogous to the $F^-(ROH)_n$ clusters, the $-\Delta H^o$ values for the $Cl^- + ROH \rightleftharpoons Cl^-(ROH)$ clustering equilibria increase going from R = Me to *t*-Bu. In Table 2, data from both the present work and literature values are shown for the different chloride alcohol clusters.

The $Cl^- + CH_3OH \rightleftharpoons Cl^-(CH_3OH)$ equilibrium is a system that has been studied extensively [2–4,7,9,26]. The present value of $\Delta H^o = -17.5 \pm 0.3$ kcal mol^{-1} is in excellent agreement with most other PHPMS determinations [4,7,9]. Kebarle's HPMS value is definitely too low [2,3], whereas Larson and McMahon's estimated ICR value of -16.8 kcal mol^{-1} is in reasonable agreement [26]. The value by Yang et al. of -18.7 kcal mol^{-1} determined by EPDS seems too high compared to most other values [35]. The observed trend in $\Delta H^o_{0,1}$ going from R = Me to *t*-Bu can be explained by an increase in the polarizability of the alcohol molecules as can be seen in Fig. 2.

For R = *i*-Pr the literature values of ΔH^o and ΔS^o [7,26] are somewhat smaller than those from the present work, while Yamdagni et al. find values for R = *t*-Bu that are very different from the present work [2].

The deprotonation enthalpy of HCl is much smaller than the gas phase acidities of the four alcohol molecules [68,69] and consequently Cl^- (HOR) are the only qualitatively correct representations for these systems. Larson and McMahon found that for both F^- (HOR) and Cl^- (HOR) systems, there are linear relationships between the deprotonation enthalpy difference of ROH and HF or HCl [$(\Delta H_{acid}(ROH) - \Delta H_{acid}(HX)$ or $\Delta\Delta H_{acid}$, X = F, Cl] and the negative standard enthalpy change for the $X^- + ROH \rightleftharpoons X^-(ROH)$ (X = F, Cl) clustering equilibria [26,27]. The present work also found a similar linear relationship for X = F and an identical one seems to apply for X = Cl, Br, and I as well.

It is surprising to observe in the same figure that the corresponding data for CN^- clustering onto the different alcohols and water [70] shows a linear correlation with an identical slope as for the four halides. In general, CN^- and Cl^- bind nearly identically [71]. The difference in this case might be caused by the occurrence of binding through the carbon atom instead of the nitrogen atom [70]. This can be explained by the fact that the deprotonation enthalpies of HNC and HCl are very similar, but different from HCN [70].

It has been suggested that in the $Cl^-(CH_3OH)$ complex, there is not only an interaction between Cl^- and H–OCH_3, but also between Cl^- and H–CH_2OH [25,30]. The latter is mainly caused by the size of chloride, which gives rise to a nonlinear CH_3O–$H \cdots Cl^-$ bond angle [23,30,36]. This is very different from $F^-(CH_3OH)$, where the CH_3O–$H \cdots F^-$ bond angle is almost linear [30,36,38,49]. The bidentate interaction between Cl^- and CH_3OH will give rise to more hindered rotation of the methyl group at very low temperatures. This hindered rotation around the C–O bond is expected to be more prominent in the cases where R = Et, *i*-Pr, and *t*-Bu. It is hard to give a magnitude of the actual contribution of the $Cl^- \cdots$ H–CH_2OH interaction. Some insight may be gained from the $Cl^- + (CH_3)_2O \rightleftharpoons Cl^{-\cdot}(CH_3)_2O$ equilibrium studied by PHPMS, which yielded $\Delta H^o = -7.5 \pm 0.2$ kcal mol^{-1} and $\Delta S^o = -15.3 \pm 0.5$ cal mol^{-1} K^{-1} [72]. The ΔH^o value is almost identical to the theoretical value obtained by Smith et al. [73]. At the MP2[cc-pVTZ+3*s*3*p*2*d*/D95+**]//MP2[D95+*/D95+**] level of theory, they obtained an ion–molecule complexation energy of -7.56 kcal mol^{-1}. This result shows clearly that the $Cl^- \cdots$ H–CH_2OH interaction is expected to be relatively small. For R = Et, *i*-Pr, and *t*-Bu, the

$Cl^- \cdots H$–C interaction is expected to be somewhat stronger, mainly because of the shorter distance between the chloride and the methyl hydrogen atom. This seems to be reflected in the ΔS^o values for the $Cl^- + ROH \rightleftharpoons Cl^-(ROH)$ equilibrium clustering reactions. Going from R = Me to *t*-Bu, $-\Delta S^o$ increases as it did for the fluoride alcohol clusters and the values are of the same magnitude. The fact that the $Cl^- \cdots H$–OR bond is less strong than the $F^- \cdots H$–OR bond might be partly compensated for by a somewhat stronger $Cl^- \cdots H$–C bond compared to the $F^- \cdots H$–C bond.

Surprisingly, only two theoretical studies on $Cl^-(CH_3OH)$ have been published in the literature. Hiraoka's ab initio molecular orbital calculations at the HF/3-21G+d(0.75) level of theory found a methanol chloride affinity of 16.2 kcal mol^{-1} [30] and this value seems to be too low compared to the PHPMS and ICR data. Recently, Berthier et al. calculated the binding energies of the Cl^- onto methanol [23]. Their calculations were performed at the MP2 and MP4 levels of theory, by using extended Gaussian basis sets enlarged with both standard valence and semi-diffuse coulomb polarization orbitals. At the highest levels used, the chloride affinity of methanol was calculated to be 17.5 kcal mol^{-1} (14.9 kcal mol^{-1}, including the basis set superposition error (BSSE) correction).

Xantheas calculated at the MP2/aug-cc-pVDZ level of theory the normal vibrational frequencies of $Cl^-(H_2O)_n$ clusters (n = 1–3) [48] and in order to rationalize entropy trends in a qualitative manner, a similar discussion as for the fluoride water clusters can be given by using the abovementioned data.

The $Cl^-(ROH) + ROH \rightleftharpoons Cl^-(ROH)_2$ clustering equilibria show identical trends as the $F^-(ROH) + ROH \rightleftharpoons F^-(ROH)_2$ series. Going from R = Me to *t*-Bu, both $-\Delta H^o$ and $-\Delta S^o$ will increase. It may be speculated that the increase in $-\Delta S^o$ is mainly because of a change in the standard vibrational entropy, ΔS^o_V, caused by low frequency intermolecular and intramolecular vibrations. Calculations by Xantheas at the MP2/aug-cc-pVDZ level of theory show that by going from $Cl^-(H_2O)$ to $Cl^-(H_2O)_2$, two new normal vibrational modes with frequencies smaller than 200 cm^{-1} are introduced [48]. It is very likely that there will also be a minor contribution from the change in the standard rotational entropy, ΔS^o_V, predominantly caused by hindering of internal methyl group rotations.

In light of the possibility that the methanol molecules are fairly mobile, other structures were examined. For the disolvated chloride two structures were calculated that are displayed in Figs. 6(b) and (c). The structure that has hydrogen bonding between the two methanol molecules, although only one methanol is directly interacting with the chloride, has an energy that is within 1 kcal mol^{-1} of the central halide structure (Table 7). This result makes both isomers competitive. These are only preliminary results, but they illustrate quite clearly that for multiple solvated halide alcohol clusters, several isomers might contribute to the experimentally measured enthalpy and entropy. Consequently, a discussion on trends for enthalpy and entropy might have to be expanded to include these hydrogen-bonded isomers (see below).

The ΔH^o values of the $Cl^-(ROH)_2 + ROH \rightleftharpoons Cl^-(ROH)_3$ clustering equilibria show the expected decreasing trend going from R = Me to *t*-Bu. For R = Me the value is very close to the PHPMS value by Evans et al. [9] (−10.5 versus −10.8 kcal mol^{-1}), but both are somewhat smaller than Hiraoka's PHPMS value of −11.8 kcal mol^{-1} [7]. For R = Et to *t*-Bu, the ΔH^o values obtained by the present work are systematically somewhat larger than the literature values [7]. The observed trend is very similar to the trends observed for the Cl^-/ROH/(0,1) and (1,2) clustering equilibria.

From molecular beam depletion spectroscopy [74,75], infrared photodissociation experiments [76,77], and theoretical calculations [78–80] it has been shown that for the neutral methanol trimer, the lowest energy configuration has a planar ring structure. This may also be true for the neutral ethanol trimer. For the *iso*-propanol trimer it is hard to say and it definitely seems very unlikely for the neutral *tert*-butanol trimer [81]. Weinheimer and Lisy showed by VPDS experiments that for both the $Cs^+(H_2O)_3$ [82] and $Cs^+(CH_3OH)_3$ clusters [83], two

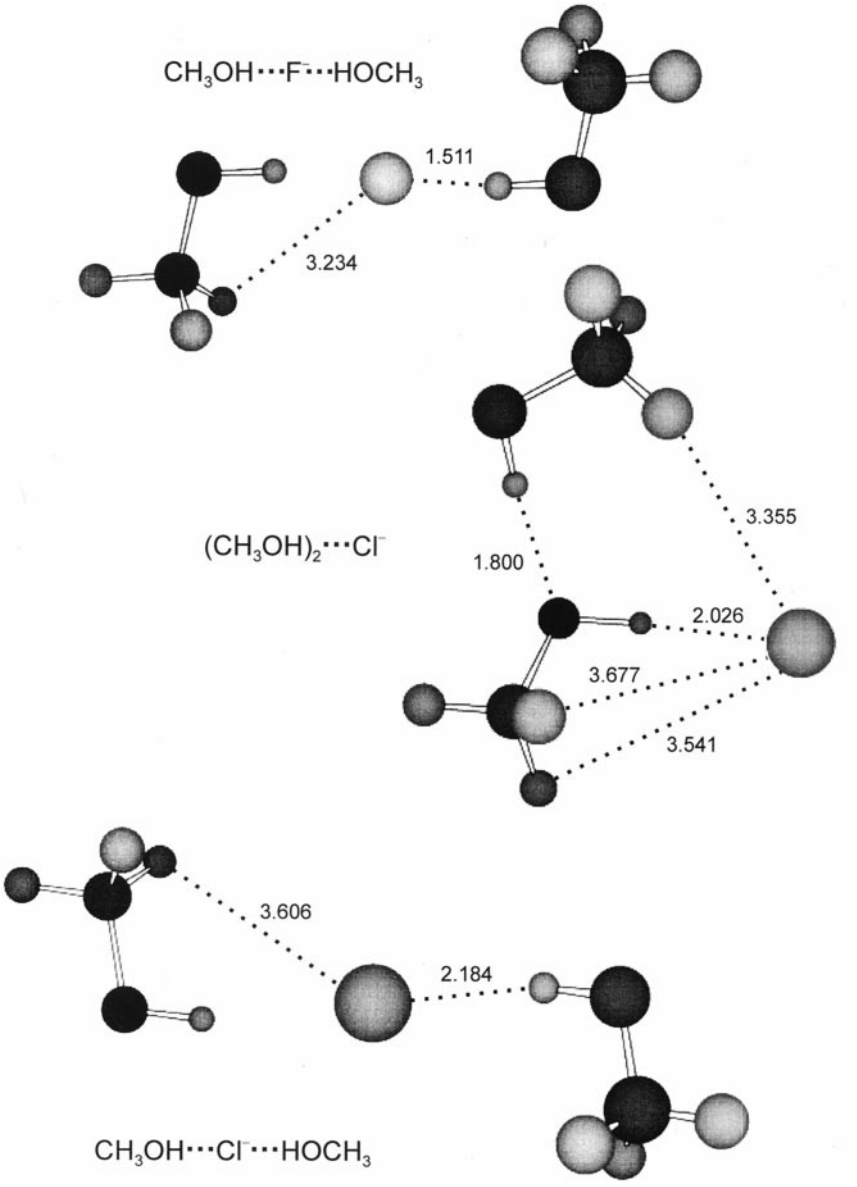

Fig. 6. Optimized geometries at the DFT B3LYP/6–311+G(*d*, *p*) level of theory for: (a) $F^-(CH_3OH)_2$, (b) $Cl^-(CH_3OH)_2$, (c) $Cl^-(CH_3OH)(CH_3OH)$ (all distances in Å).

structural isomers exist simultaneously. It seems reasonable to speculate that perhaps for the $X^-(ROH)_3$ (X = Cl, Br, I; R = Me, Et, *i*-Pr) clusters, structural isomers are possible and actually exist [81,84]. Whether they are, in fact, generated in the high pressure ion source environment is another question. The binding energy of the neutral methanol trimer, with respect to three nonbonding methanol molecules, is calculated to be -16.0 kcal · mol^{-1}, as shown in Eq. (10) [80]. By the present study it was determined that three methanol molecules bind to iodide with an enthalpy of -29.1 kcal · mol^{-1}, see eq. (11). This equation assumes that the three methanol molecules will bind equivalently to iodide.

$$3\ CH_3OH \rightleftharpoons (CH_3OH)_3 \quad (10)$$

$$\Delta H^o = -16.0\ \text{kcal mol}^{-1}$$

$$I^- + 3\ CH_3OH \rightleftharpoons I^-(CH_3OH)_3 \quad (11)$$

$$\Delta H^o = -29.1\ \text{kcal mol}^{-1}$$

By using PHPMS experiments, it will be impossible to measure the enthalpy change of iodide binding to a neutral methanol trimer [eq. (12)].

$$I^- + (CH_3OH)_3 \rightleftharpoons I^-(CH_3OH)_3 \quad (12)$$

The $I^-(CH_3OH)\ (CH_3OH)_2$ complex is, of course, also a possibility that may not be ruled out. As mentioned before for Eq. (12), the standard enthalpy change for the formation of $I^-(CH_3OH)\ (CH_3OH)_2$ from $I^-(CH_3OH)$ and $(CH_3OH)_2$ is unknown for Eq. (13).

$$I^-(CH_3OH) + (CH_3OH)_2 \rightleftharpoons I^-(CH_3OH)(CH_3OH)_2 \quad (13)$$

VPDS experiments on halide alcohol clusters will be an excellent method to investigate this. The results may give more insight into the origin of the entropy values [81]. Recently, Okumura and coworkers observed both hydrogen-bonded and free OH stretch modes of $Cl^-(H_2O)_n$ (n = 1–5) by VPDS [42].

The $-\Delta S^o$ values for the four different $Cl^-(ROH)_2 + ROH \rightleftharpoons Cl^-(ROH)_3$ clustering equilibria increase going from R = Me to *t*-Bu. Compared to the literature values, the present work gives ΔS^o values that seem too low. For R = Et to *t*-Bu, the $-\Delta S^o$ values are larger than the literature data [3,7,9]. From other data it could already be concluded that there is quite a spread in the ΔS^o values of the investigated systems. This is not surprising, considering the uncertainties in the standard entropy changes. As a consequence, making quantitative comparisons of the different data sets is a speculative exercise.

In Table 3 the results for the $Br^-(ROH)_n + ROH \rightleftharpoons Br^-(ROH)_{n+1}$ clustering equilibria are shown, including the surprisingly few literature values as well. As shown previously for the corresponding fluoride and chloride alcohol clusters, there will be a slight increase in $-\Delta H^o$ going from R = Me to *t*-Bu for $Br^- + ROH \rightleftharpoons Br^-(ROH)$. In Fig. 2 it can be seen that for Br^- and I^- there is not an identical linear relationship between α and $\Delta H^o_{0,1}$ (X^- ROH) as for F^- and Cl^-. For Br^- and I^-, the standard enthalpy changes are more or less constant for all four alcohol molecules. This can be explained by the fact that the halides become polarized by the permanent electric dipole moment of the alcohol molecule. As expected, $-\Delta H^o$ decreases going from (0,1) to (2,3), but the change is smaller than for F^- and Cl^-. This is not surprising, considering the radius of Br^-. This larger radius may give rise to both a weaker $Br^- \cdots H–OR$ and $Br^- \cdots H–C$ interaction compared to Cl^-, mainly caused by the larger distance. Consequently, the intermolecular frequencies might shift to lower values and the $–CH_3$ rotations may become less hindered. When $-\Delta S^o$ values are compared for chloride and bromide alcohol clusters, it can be seen that, in general, they are larger for Cl^- than for Br^-. This means that the above-stated hypothesis seems quite reasonable. The $-\Delta S^o$ values for the different $Br^-(ROH)_n + ROH \rightleftharpoons Br^-(ROH)_{n+1}$ clustering equilibria are, in general, more or less constant for n = 0–2. This might be interpreted in a sense that all alcohol molecules bind in a more similar manner to bromide than they do to chloride.

Tanabe et al. calculated the vibrational frequencies of $Br^-(CH_3OH)$ at the MP4-SDTQ/MP2-D95 level of theory [34]. Three vibrations were calculated to be below 200 cm^{-1} (88, 100, and 169 cm^{-1}). The bromide affinity of methanol [$-\Delta H^o_{298\ K}$] was calculated to be 12.9 kcal mol^{-1}, close to 12.3 kcal mol^{-1} that was calculated by using the DFT B3LYP/6-311+G(d,p) level of theory. Both values are less negative than all experimentally determined values [30,35]. The G2 value of 13.5 kcal mol^{-1} is much closer to the experimental value than the present DFT result and the Tanabe et al. result.

For $Br^-(H_2O)_n$ clusters, it has been shown by performing molecular dynamics simulations, that these systems can be represented by bromide lo-

cated on a water cluster surface [46]. This is mainly because of the large radius of Br^-. Alcohol molecules are also able to form hydrogen bonded networks like water molecules do, although less extensive [80].

For the $I^- + ROH \rightleftharpoons I^-(ROH)$ clustering equilibria, a similar trend is observed as for the three other halides. The values of ΔH^o in Table 4 are in absolute magnitude smaller than the corresponding Br^- value for all four alcohol molecules. The larger radius of I^- compared to Br^- is mainly responsible for this. Except for the $I^-/CH_3OH/(0, 1)$ system, the present values of ΔH^o are larger than the PHPMS data by Caldwell et al. and Hiraoka and co-workers [5,30]. The EPDS ΔH^o value of -14.4 kcal mol^{-1} definitely seems too large [35]. Going from R = Me to Et, Caldwell et al. observed a small increase in $-\Delta H^o$, whereas for R = Et to *t*-Bu it remains constant. A similar trend is observed in this work, except the absolute magnitudes are larger. The FT-ICR value for ΔH^o of -14.4 kcal mol^{-1} for R = Et by Tanabe et al. also seems too small for what might be expected. These authors mentioned that especially adducts of Br^- and I^- with large neutral molecules readily undergo dissociation induced by thermal radiation in the FT-ICR cell [85–88]. This may introduce some extra uncertainties in these values. Except for R = Me, no data in the literature are available for the (1,2) and (2,3) clustering equilibria. For R = Me, the $-\Delta H^o$ values obtained from Hiraoka's PHPMS experiments [30] are larger than our present data, although both sets of data show more or less similar trends.

Going from R = Me to *t*-Bu, $-\Delta H^o$ increases for both the (1,2) and (2,3) equilibria. The increases are smaller than for the corresponding Br^- data, mainly because of the larger I^- radius. In the $I^-(ROH)_{2/3}$ clusters, the alcohol molecules are probably very mobile, mainly because of the small binding enthalpies. The presence of equivalent alcohol molecules within the iodide alcohol clusters is a reasonable possibility. The occurrence of neutral dimers and trimers within the reservoir and high pressure ion source seems very unlikely, especially at the temperatures used for most experiments.

For the $I^-(ROH)_n + ROH \rightleftharpoons I^-(ROH)_{n+1}$ clustering equilibria measured, in general, the $-\Delta S^o$ values increase going from R = Me to *t*-Bu. For all four alcohols used, $-\Delta S^o$ decreases going from (0,1) to (2,3). Hiraoka and co-workers observed that for R = Me going from (1,2) to (2,3), ΔS^o remains more or less constant [30]. For (0,1) to (1,2), on the other hand, they observed quite an increase in $-\Delta S^o$. Our ΔS^o values for the (0,1) equilibria are, in general, larger than the data by Caldwell and Hiraoka [5,30]. The lack of theoretical calculations makes it very hard to speculate on the relative contributions to the entropy changes within the $I^-(ROH)_n$ complexes. It seems reasonable to assume that the changes in the rotational and vibrational entropy will be small. This is mainly due to the weak $I^- \cdots H–C$ and $I^- \cdots H–OR$ bonds. The assumed relative high mobility of the alcohol molecules might result in smaller than expected entropy changes.

5. Conclusion

In this paper we have presented the results from both experimental and computational work on halide alcohol clusters. The data for systems previously investigated by other groups are, in general, confirmed by the present study. For the higher order F^-, Br^-, and I^- alcohol clusters, no reference data were present. The consistency in the observed trends gave us confidence that these new values are of the proper magnitude.

The trend in ΔH^o going from R = Me to *t*-Bu can be rationalized by an increase of the alcohol polarizability in the ion-induced dipole term. For X = F to I, $-\Delta H^o$ decreases mainly because of the increased halide radius. By addition of more ligands, $-\Delta H^o$ decreases mainly by a larger dipole-dipole interaction between the alcohol molecules.

In addition, a linear correlation has been found between the gas phase acidity differences of ROH and HX [$\Delta H_{acid}(ROH) - \Delta H_{acid}(HX)$] for X = F, Cl, and Br and all four alcohols, and the negative standard enthalpy changy of the association reaction $X^- + ROH \rightleftharpoons X^-(ROH)$ [$-\Delta H^o_{0,1}(X^-/ROH)$]. This cor-

Table 9
Summary of experimental and calculated entropy changes for some selected halide alcohol clustering equilibria

X	ROH	$(n,n+1)$	ΔS^{o} [a]		Calculated ΔS^{o} [a]		
			Experimental	Calculated	ΔS^{o}_{trans}	ΔS^{o}_{rot}	ΔS^{o}_{vib}
F	CH_3OH	(0,1)	−23.4 ± 1.2	−22.6	−33.3	+4.4	+6.3
F	CH_3OH	(1,2–2)	−24.6 ± 0.8	−23.4	−34.8	−16.4	+27.8
Cl	CH_3OH	(0,1)	−24.0 ± 0.7	−19.2	−34.4	+5.9	+9.3
Cl	CH_3OH	(1,2–2)	−22.8 ± 1.1				
Cl	CH_3OH	(1,2–1)		−29.6	−35.1	−15.2	+20.7
Br	CH_3OH	(0,1)	−21.9 ± 0.4	−19.5	−35.4	+6.7	+9.2
Br	C_2H_5OH	(0,1)	−19.8 ± 0.4	−20.0	−36.1	+4.8	+11.3

[a] cal mol^{-1} K^{-1}.

relation suggests the occurrence of a single well potential energy surface.

The trends in ΔS^{o} by changing the halide, the alcohol, or the number of ligands in the cluster have been discussed in a more qualitative manner. These trends can be understood by considering the presence of low frequency intermolecular vibrations and hindered internal rotations.

In addition, calculations at the DFT B3LYP/6-311+G(d,p) and G2 levels have been performed on a number of selected clusters to gain more insight. In general, the results obtained by this level of theory were good enough to qualitatively discuss the experimental results.

Acknowledgements

B.B. would like to acknowledge the University of Waterloo for the International Graduate Student Scholarship provided, and Jakob Felding for assistance with the CD_3OH synthesis. T.B.M. gratefully acknowledges the Natural Sciences and Engineering Research Council of Canada (NSERC) for financial support.

References

[1] M. Arshadi, R. Yamdagni, P. Kebarle, J. Phys. Chem. 74 (1970) 1475.
[2] R. Yamdagni, P. Kebarle, J. Am. Chem. Soc. 93 (1971) 7139.
[3] R. Yamdagni, J.D. Payzant, P. Kebarle, Can. J. Chem. 51 (1973) 2507.
[4] R.G. Keesee, A.W. Castleman Jr., Chem. Phys. Lett. 74 (1980) 139.
[5] G. Caldwell, P. Kebarle, J. Am. Chem. Soc. 106 (1984) 967.
[6] L.W. Sieck, J. Phys. Chem. 89 (1985) 5552.
[7] K. Hiraoka, S. Mizuse, Chem. Phys. 118 (1987) 457.
[8] K. Hiraoka, S. Mizuse, S. Yamabe, J. Phys. Chem. 92 (1988) 3943.
[9] D.H. Evans, R.G. Keesee, A.W. Castleman Jr., J. Phys. Chem. 95 (1991) 3558.
[10] H. Kistenmacher, H. Popkie, E. Clementi, J. Chem. Phys. 58 (1973) 5627.
[11] H. Kistenmacher, H. Popkie, E. Clementi, J. Chem. Phys. 59 (1973) 5842.
[12] A. Beyer, A. Karpfen, P. Schuster, Chem. Phys. Lett. 67 (1979) 369.
[13] R. Janoschek, J. Mol. Struct. 84 (1982) 237.
[14] A.M. Sapse, D.C. Jain, Int. J. Quant. Chem. 27 (1985) 281.
[15] J. Gao, D.S. Garner, W.L. Jorgensen, J. Am. Chem. Soc. 108 (1986) 4784.
[16] S.S. Sung, P.C. Jordan, J. Chem. Phys. 85 (1986) 4045.
[17] B.F. Yates, H.F. Schaefer III, T.J. Lee, J.E. Rice, J. Am. Chem. Soc. 110 (1988) 6327.
[18] S. Lin, P.C. Jordan, J. Chem. Phys. 89 (1988) 7492.
[19] G. Alagona, C. Ghio, Z. Latajka, J. Tomasi, J. Phys. Chem. 94 (1990) 2267.
[20] X.G. Zhao, A. Gonzales-Lafont, D.G. Truhlar, R. Steckler, J. Chem. Phys. 94 (1991) 5544.
[21] J.E. Combariza, N.R. Kestner, J. Jortner, Chem. Phys. Lett. 203 (1993) 423.
[22] L.S. Sremaniak, L. Perera, M.L. Berkowitz, Chem. Phys. Lett. 218 (1994) 377.
[23] G. Berthier, R. Savinelli, A. Pullman, Int. J. Quantum Chem. 63 (1997) 567.
[24] R.N. Rosenfeld, J.M. Jasinski, J.I. Brauman, Chem. Phys. Lett. 71 (1980) 400.
[25] J.W. Larson, T.B. McMahon, J. Am. Chem. Soc. 105 (1983) 2944.
[26] J.W. Larson, T.B. McMahon, J. Am. Chem. Soc. 106 (1984) 517.
[27] C.R. Moylan, J.A. Dod, J.I. Brauman, Chem. Phys. Lett. 118 (1995) 38.

[28] C.R. Moylan, J.A. Dodd, C.C. Han, J.I. Brauman, J. Chem. Phys. 86 (1987) 5350.
[29] J.E. Szulejko, F.E. Wilkinson, T.B. McMahon, Proceedings of the 37th ASMS Conference on Mass Spectrometry and Allied Topics, May 21–26, 1989, Miami Beach, FL, p. 333.
[30] K. Hiraoka, S. Yamabe, Int. J. Mass Spectrom. Ion Processes 109 (1991) 133.
[31] F.E. Wilkinson, J.E. Szulejko, C.E. Allison, T.B. McMahon, Int. J. Mass Spectrom. Ion Processes 117 (1992) 487.
[32] D.M. Peiris, J.M. Riveros, J.R. Eyler, Int. J. Mass Spectrom. Ion Processes 159 (1996) 169.
[33] J.E. Mihalick, G.G. Gatev, J.I. Brauman, J. Am. Chem. Soc. 118 (1996) 12424.
[34] F.K.J. Tanabe, N.H. Morgan, J.M. Riveros, J. Phys. Chem. 100 (1996) 2862.
[35] Y. Yang, H.V. Linnert, J.M. Riveros, K.R. Williams, J.R. Eyler, J. Phys. Chem. A 101 (1997) 2371.
[36] F.E. Wilkinson, M. Peschke, J.E. Szulejko, T.B. McMahon, Int. J. Mass Spectrom. 175 (1998) 225.
[37] J.F.G. Faigle, P.C. Isolani, J.M. Riveros, J. Am. Chem. Soc. 98 (1976) 2049.
[38] S.E. Bradforth, D.W. Arnold, R.B. Metz, A. Weaver, D.M. Neumark, J. Phys. Chem. 95 (1991) 8066.
[39] G. Markovich, S. Pollack, R. Giniger, O. Cheshnovsky, J. Chem. Phys. 101 (1994) 9344.
[40] C. Bässmann, U. Boesl, D. Yang, G. Drechsler, E.W. Schlag, Int. J. Mass Spectrom. Ion Processes 159 (1996) 153.
[41] M.S. Johnson, K.T. Kuwata, C.-K. Wong, M. Okumura, Chem. Phys. Lett. 260 (1996) 551.
[42] J.-H. Choi, K.T. Kuwata, Y.-B. Cao, M. Okumura, J. Phys. Chem. A 102 (1998) 503.
[43] T. Asada, K. Nishimoto, K. Kitaura, J. Phys. Chem. 97 (1993) 7724.
[44] J.E. Combariza, N.R. Kestner, J. Jortner, J. Chem. Phys. 100 (1994) 2851.
[45] S.S. Xantheas, T.H. Dunning Jr., J. Phys. Chem. 98 (1994) 13489.
[46] I. Tuñón, M.T.C. Martins-Costa, C. Millot, M.F. Ruiz-López, Chem. Phys. Lett. 241 (1995) 450.
[47] S.S. Xantheas, L.X. Dang, J. Phys. Chem. 100 (1996) 3989.
[48] S.S. Xantheas, J. Phys. Chem. 100 (1996) 9703.
[49] B.D. Wladkowski, A.L.L. East, J.E. Mihalick, W.D. Allen, J.I. Brauman, J. Chem. Phys. 100 (1994) 2058.
[50] J.E. Szulejko, J.J. Fisher, T.B. McMahon, J. Wronka, Int. J. Mass Spectrom. Ion Processes 83 (1988) 147.
[51] J.E. Szulejko, T.B. McMahon, Int. J. Mass Spectrom. Ion Processes 109 (1991) 279.
[52] P. Kebarle, Techniques for the Study of Ion-Molecule Reactions (Techniques of Chemistry), W. Saunders, J.M. Farrer (Eds.), Wiley-Interscience, New York, 1988.
[53] M. Meot-Ner (Mautner), L.W. Sieck, Int. J. Mass Spectrom. Ion Processes 109 (1991) 187.
[54] L.A. Curtiss, K. Raghavachari, P.C. Redfern, J.A. Pople, J. Chem. Phys. 106 (1997) 1063.
[55] For an explanation and leading references, see W.J. Hehre, L. Radom, P.v.R. Schleyer, Ab Initio Molecular Orbital Theory, Wiley, New York, 1986.
[56] M.J. Frisch, G.W. Trucks, H.B. Schlegel, P.M.W. Gill, B.G. Johnson, M.A. Robb, J.R. Cheeseman, T. Keith, G.A. Petersson, J.A. Montgomery, K. Raghavachari, M.A. Al-Laham, V.G. Zakrzewski, J.V. Ortiz, J.B. Foresman, C.Y. Peng, P.Y. Ayala, W. Chen, M.W. Wong, J.L. Andres, E.S. Replogle, R. Gomperts, R.L. Martin, D.J. Fox, J.S. Binkley, D.J. Defrees, J. Baker, J.P. Stewart, M. Head-Gordon, C. Gonzalez, J.A. Pople, GAUSSIAN 94, Revision B.3, Gaussian, Inc., Pittsburgh, PA, 1995.
[57] T. Su, M.T. Bowers, Int. J. Mass Spectrom. Ion Phys. 12 (1973) 347.
[58] J.J. Grabowski, V.M. Bierbaum, C.H. DePuy, J. Am. Chem. Soc. 105 (1983) 2565.
[59] CRC Handbook of Chemistry and Physics, Ref. Data, 76th ed., D.R. Lide, (Ed). CRC, Boca Raton, FL, 1995, pp. 9–42/50, 10–196, 10–202/204, 12–14.
[60] T.H. Lowry, K. Schueller Richardson, Mechanism and Theory in Organic Chemistry, 3rd ed., Harper and Row, New York, 1987, pp. 178–179.
[61] W. Zhang, Ch. Beglinger, J.A. Stone, J. Phys. Chem. 99 (1995) 11673.
[62] K. Norrman, T.B. McMahon, J. Am. Chem. Soc. 118 (1997) 2449.
[63] C. Li, P. Ross, J.E. Szulejko, T.B. McMahon, J. Am. Chem. Soc. 118 (1996) 9360.
[64] S.L. Gong, R.E. Jervis, J. Chem. Phys. 103 (1995) 7081.
[65] F. Bouchard, V. Brenner, C. Carra, J.W. Hepburn, G.K. Koyanagi, T.B. McMahon, G. Ohanessian, M. Peschke, J. Phys. Chem. A 101 (1997) 5885.
[66] D. Stöckigt, Chem. Phys. Lett. 250 (1996) 387.
[67] This problem has been noted before [65]. Because the energy barriers will be very low (less than 0.5 kcal mol^{-1}), one way to view the problem is to note that under most experimental conditions, the average will be the one that has been calculated.
[68] S.G. Lias, J.E. Bartmess, J.F. Liebman, J.L. Holmes, R.D. Levin, W.G. Mallard, J. Phys. Chem. Ref. Data 17 (1998) (Suppl 1).
[69] http://webbook.nist.gov./chemistry/ion.
[70] J.W. Larson, J.E. Szulejko, T.B. McMahon, J. Am. Chem. Soc. 110 (1988) 7604.
[71] T.B. McMahon, J.W. Larson, J. Am. Chem. Soc. 109 (1987) 6230.
[72] J.E. Szulejko, B. Bogdanov, M. Peschke, T.B. McMahon, Proceedings of the 40th ASMS Conference on Mass Spectrometry and Allied Topics, May 31–June 4, 1998, Orlando, FL, p. 444.
[73] G.D. Smith, R.L. Jaffe, H. Partridge, J. Phys. Chem. A 101 (1997) 1705.
[74] F. Huisken, A. Kulcke, C. Laush, J.M. Lisy, J. Chem. Phys. 95 (1991) 3924.
[75] F. Huiskens, M. Kaloudis, M. Koch, O. Werhahn, J. Chem. Phys. 105 (1996) 8965.
[76] U. Buck, X.J. Gu, Ch. Lauenstein, A. Rudolph, J. Chem. Phys. 92 (1990) 6017.
[77] U. Buck, I. Ettischer, J. Chem. Phys. 108 (1998) 33.
[78] O. Mó, M. Yáñez, J. Elguero, J. Mol. Struct. (Theochem.) 314 (1994) 73.
[79] A. Bleiber, J. Sauer, Chem. Phys. Lett. 28 (1995) 243.

[80] U. Buck, J.G. Siebers, R.J. Wheatley, J. Phys. Chem. 108 (1998) 20.
[81] J.M. Lisy, personal communication.
[82] C.J. Weinheimer, J.M. Lisy, J. Chem. Phys. 105 (1996) 2938.
[83] C.J. Weinheimer, J.M. Lisy, Int. J. Mass Spectrom. Ion Processes 159 (1996) 197.
[84] O.M. Cabarcos, C.J. Weinheimer, T.J. Martinez, J.M. Lisy, unpublished.
[85] D. Thölmann, D.S. Tonner, T.B. McMahon, J. Phys. Chem. 98 (1994) 2002.
[86] M. Sena, J.M. Riveros, Rapid Commun. Mass Spectrom. 8 (1994) 1031.
[87] R.C. Dunbar, J. Phys. Chem. 98 (1994) 8705.
[88] R.C. Dunbar, T.B. McMahon, D. Thölmann, D.S. Tonner, D.R. Salahub, D. Wei, J. Am. Chem. Soc. 117 (1995) 12819.
[89] P. Kebarle, Annu. Rev. Phys. Chem. 28 (1977).
[90] A. Batana, J. Bruno, R.W. Munn, Mol. Phys. 92 (1997) 1029.